Understanding the strong coupling limit of the $\mathcal{N}=4$ supersymmetric Yang-Mills theory at finite temperature

Edward Shuryak and Ismail Zahed
Department of Physics and Astronomy, State University of New York, Stony Brook, New York 11794, USA
(Received 13 August 2003; published 27 February 2004)

Recently, a number of intriguing results have been obtained for strongly coupled $\mathcal{N}=4$ supersymmetric Yang-Mills theory in vacuum and matter, using the AdS-CFT correspondence. In this work, we provide a physical picture supporting and explaining most of these results within the gauge theory. The modified Coulomb's law at strong coupling forces static charges to communicate via the high frequency modes of the gauge or scalar fields. Therefore, the interaction between even relativistically moving charges can be approximated by a potential. At strong coupling, WKB arguments yield a series of deeply bound states, whereby the large Coulomb attraction is balanced by centrifugation. The result is a constant density of light bound states at *any* value of the strong coupling, explaining why the thermodynamics and kinetics are coupling constant independent. In essence, at strong coupling the matter is not made of the original quasiparticles but of much lighter (binary) composites. A transition from weak to strong coupling is reminiscent of a transition from high to low temperature in QCD. We establish novel results for screening in vacuum and matter through a dominant set of diagrams some of which are in qualitative agreement with known strong coupling results.

DOI: 10.1103/PhysRevD.69.046005 PACS number(s): 11.25.Mj, 11.10.Wx, 12.38.Mh

I. INTRODUCTION

$\mathcal{N}=4$ super-Yang-Mills (SYM) theory is the most famous example of a conformal field theory (CFT) in 4 dimensions. This theory has a zero beta function and a nonrunning coupling constant, which can be continuously changed from weak to strong. Unlike QED or QCD, where for a critical coupling $\alpha\approx 1$ there is vacuum rearrangement, CFT is believed to remain in the same Coulomb (plasmalike) phase for all couplings, even strong ones $\lambda=g^2N_c\gg 1$. Thus, it provides an interesting theoretical laboratory for understanding properties of a strongly coupled quark-gluon plasma (QGP) in QCD, which occurs in and around the critical temperature T_c, as discussed in our recent paper [1].

A key breakthrough in making the results of the strong coupling regime within reach was the AdS-CFT correspondence suggested by Maldacena [2]. This conjecture has turned the intricacies of strong coupling gauge theories into a classical problem in gravity, albeit in 10 dimensions, leading to the static heavy-quark potential [2–4], small angle scattering [5,6] and large angle scattering [7]. For instance, the static potential between a heavy quark and antiquark follows from a minimal surface (classical string) between the quarks streched by gravity (metric of the AdS space) as depicted in Fig. 1(a). The result is a modified Coulomb law [2,3]:

$$V(L)=-\frac{4\pi^2}{\Gamma(1/4)^4}\frac{\sqrt{\lambda}}{L} \tag{1}$$

for $\lambda\gg 1$. The numerical coefficient in the first bracket is 0.228. The latter will be compared to the result from a diagrammatic resummation below.

The case of nonzero temperature is represented in the AdS space by the occurence of a black hole in the 5th dimension, whereby its Schwarchild radius is identified with the inverse temperature. When the string between charges extends all the way to the black hole as shown in Fig. 1(b), the heavy quark potential is totally screened for a Debye radius of order $1/T$ [3]. This is to be contrasted with $1/\sqrt{\lambda}T$ expected in the weak coupling limit for the electric modes, and $1/\lambda\ T$ for the magnetic modes.

The AdS-CFT correspondence was also used to generate a number of finite temperature results at strong coupling, including the free energy [8], the electric Debye screening [4], and the viscosity [9]. Also a number of real-time correlators were recently investigated, leading a tower of equidistant but unstable resonances [10,11]. Their origin remains a mystery which we will attempt to explain.

The main puzzle related with all these results whether it is the free energy, the viscosity, or the resonance frequencies is their independence on the coupling λ in strong coupling. We recall that the interaction between the (quasi) particles such as Eq. (1) is proportional to $\sqrt{\lambda}$, and the strong-couping Debye distance is $1/r\sim T$, so the relevant quasiparticle energy scale must be $\sqrt{\lambda}T$. In a naive picture of matter being essentially a plasma of quasiparticles (weak coupling) one would expect the interaction terms of such order to show up in the free energy.

The main objective of this paper is to explain this puzzle, in the process of which novel results will also be derived. This is achieved in two major steps as we now detail.

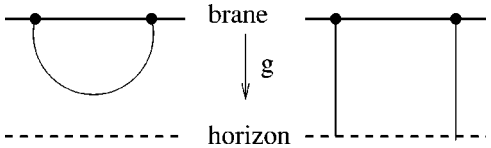

FIG. 1. Two types of solutions describing the potential between two static charges (large dots) in the ordinary $4d$ space (on the D3 brane). The string originating from them can either connect them (a) or not (b). In both cases the string is deflected by a background metric (the gravity force indicated by the arrow marked g) downward, along the 5th coordinate. After the string touches the black hole horizon (b) a Debye screening of the interaction takes place.

 ©2004 The American Physical Society

(i) First, we attempt to understand the dynamical picture behind the modified Coulomb law, and its Debye-screened form at finite T and strong coupling. For that, we identify in the gauge theory a set of diagrams whose resummation can reproduce the parametric features of the above-mentioned strong coupling results. As a result, we learn an important lesson: in the strong coupling regime even the static charges communicate with each other via high frequency gluons and scalars, propagating with an effective superluminal velocity $v \approx \lambda^{1/4} \gg 1$.

(ii) Second, we argue that even for relativistically moving quasiparticles the interaction can be described by a potential with a *near-instantaneous* and *quasi-Abelian* interaction, a screened version of a modified Coulomb law given above. Solving the Klein-Gordon (or Dirac or Yang-Mills) equations for scalars (or spinors or gluons) in a WKB approximation yields *towers of deeply bound states*, extending from large quasiparticle masses $m/T \approx \sqrt{\lambda}$ all the way to small ones $E/T \approx \lambda^0$ that are independent of the coupling constant. Their existence in a strongly coupled plasma at any value of the strong coupling, explains the main puzzle mentioned above. So, the $\mathcal{N}=4$ SYM theory at finite temperature and strong coupling is *not* a gas of quasiparticles, but a gas of (much lighter) *composites*. We have found a ''precursor'' of such phenomenon in a near-critical quark-gluon plasma in QCD [1].

Before explaining these results in a technical way, let us first explain our motivations and some intuitive ideas which were important to us in deriving them. Let us first mention that Semenoff *et al.* [12] made a crucial observation: the sum of ladder-type diagrams in Feynman gauge reproduces the strong coupling results. For the circular Wilson loop the matching is exact, and is also qualitatively correct for the rectangular one, leading to the parametrically correct modified Coulomb law at strong coupling (zero temperature).

Intuitively, the reason for a potential-like regime stems from the fact that for $\lambda \gg 1$ the time between subsequent exchange of quanta is very short. The cost of the repulsive Coulomb energy becomes prohibitively large at strong coupling, forcing both charges to almost simultaneously change their colors, keeping them oriented in mutually the most attractive positions. These interactions are naturally ordered in time, justifying the use of ladder-type approximations.

We extend these observations in two important ways.

(i) First, we identify higher order diagrams which contribute equally to the potential, and those which are subleading. Although we will not attempt to sum them all, we argue that the distribution of gluons or scalars accompanying a pair of static charges look like a ''quasistring,'' with a small transverse size of order $L/\lambda^{1/4}$ in comparison to the length L.

(ii) Second, we show how Wilson loops in matter get their strong coupling Coulomb's law from an Abelianized Coulomb's law over time scales of the order of $L/\lambda^{1/4}$, using ladder diagrams. The short time scale in matter is conditioned by the high frequency modes which yield a quasistatic potential over times of order $\sqrt{L/\omega_p}$ with $\omega_p \approx \sqrt{\lambda} T$ the typical plasmon frequency.

The bulk screening in the ground state can also be characterized by the dielectric constant $\epsilon = 1 + 4\pi\, \chi_e$. The electric susceptibility follows from a simple Drude-Lorentz model where the dipole response follows from a high frequency harmonic oscillator

$$\chi_e \approx \frac{\mathbf{n}\lambda}{m\omega^2} \approx \frac{m^3 g^2}{m(m^2\sqrt{\lambda})} \approx \sqrt{\lambda}, \tag{2}$$

where all the scales are set by the condensate value $m(\lambda)$ which is seen to drop in Eq. (2). The dipole size $1/m$ is small. Thus $\epsilon \approx \sqrt{\lambda}$ and the vacuum Coulomb's law is $-\lambda/\epsilon\, L \approx -\sqrt{\lambda}/L$, the result obtained in large N_c and strong coupling.

II. DERIVING THE MODIFIED COULOMB'S LAW

We start our discussion by reminding the reader of the (Euclidean) derivation of the standard Coulomb's law between two attractive and abelian static charges. In the first quantized form in Feynman gauge one simply gets it from a 00-component of the photon (gluon) propagator

$$V(L) = -\frac{\lambda}{4\pi^2} \int_{-\infty}^{+\infty} \frac{dt}{t^2 + L^2}, \tag{3}$$

where t is the relative time separation between the two charges on their world lines. In the Abelian case whether at strong or weak coupling, the interaction takes place at all time virtualities resulting in the standard instantaneous Coulomb interaction with $V(L) \approx -\lambda/L$. The non-Abelian modified Coulomb's law (1) is seen to follow from the Abelian Coulomb's law (3) whereby the relative time interval is much shorter and of the order $L/\sqrt{\lambda} \to 0$.

The effects of retardation are best captured in covariant gauges as illustrated here. At $T=0$ Feynman gauge treats the gluons and scalars on equal footing, which makes the supersymmetric structure of the underlying $\mathcal{N}=4$ SYM theory more transparent in diagrams. However, the observation itself should of course be gauge independent. For instance, in Coulomb's gauge the same result should follow from something like

$$V(L) \approx \int_{-\infty}^{+\infty} dt\ \frac{-\lambda}{L}\ \delta(\sqrt{\lambda} t), \tag{4}$$

where the instantaneous time is rescaled by $\sqrt{\lambda}$ to account for the delay. We have not worked out how this regime is explained in other gauges.

A. Summing ladders

We start by recalling some results established in [12] at zero temperature. At large N_c (number of colors), the diagrams can be viewed as 't Hooft diagrams. An example of a ladder diagram is shown in Fig. 2(a), where the rungs can be either gluons and scalars, as both are in the adjoint representation. The first lesson is that each rung contributes a factor N_c, which however only comes from planar diagrams. It means, that in contrast to the Abelian theory, the time ordering should be strictly enforced, $s_1 > s_2 > s_3 \ldots$ and $t_1 > t_2 > t_3 \ldots$, which will be important below.

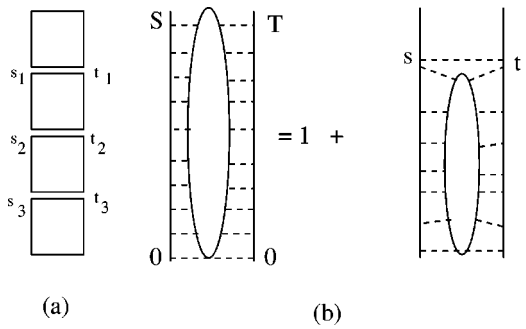

FIG. 2. (a) The color structure of ladder diagrams in the large-N_c limit: each square is a different color trace, bringing the factor N_c. The time goes vertically, and the planarity condition enforces strict time ordering, $s_1>s_2>s_3\ldots$, $t_1>t_2>t_3\ldots$. (b) Schematic representation of the Bethe-Salpeter equation (5) summing ladders.

In Fig. 2(b) we schematically depict the Bethe-Salpeter equation. The oval connected with the two Wilson lines by multiple gluon or scalar lines is the resummed Bethe-Salpeter kernel $\Gamma(s,t)$, describing the evolution from time zero to times s,t at two lines. It satisfies the following integral equation:

$$\Gamma(\mathcal{S},\mathcal{T})=1+\frac{\lambda}{4\pi^2}\int_0^{\mathcal{S}}ds\int_0^{\mathcal{T}}dt\,\frac{1}{(s-t)^2+L^2}\Gamma(s,t), \quad (5)$$

which provides the resummation of all the ladder diagrams. L is the distance between two charges, and the first factor under the integral is the (Euclidean) propagator for one extra gluon or scalar added to the ladder. The kernel obviously satisfies the boundary condition $\Gamma(\mathcal{S},0)=\Gamma(0,\mathcal{T})=1$. If the equation is solved, the ladder-generated potential follows from

$$V_{\rm lad}(L)=-\lim_{T\to+\infty}\frac{1}{\mathcal{T}}\,\Gamma\,(\mathcal{T},\mathcal{T}). \quad (6)$$

In weak coupling $\Gamma\approx 1$ and the integral on the right-hand side (RHS) is easily taken, resulting in

$$\Gamma(\mathcal{S},T\,)\approx 1+\frac{\lambda}{8\pi}\,\frac{\mathcal{S}+T}{L}, \quad (7)$$

which results into the standard Coulomb's law. Note that in this case the typical relative time difference between emission and absorption of a quantum $|t-s|\approx L$, so one can say that virtual quanta travel at a speed $v\approx 1$.

For solving it at any coupling, it is convenient to switch to the differential equation

$$\frac{\partial^2\Gamma}{\partial\mathcal{S}\,\partial\mathcal{T}}=\frac{\lambda/4\pi^2}{(\mathcal{S}-T)^2+L^2}\Gamma(\mathcal{S},T) \quad (8)$$

and change variables to $x=(\mathcal{S}-T)/L$ and $y=(\mathcal{S}+T)/L$ through

$$\Gamma(x,y)=\sum_m\ \mathbf{C}_m\gamma_m(x)e^{\omega_m y/2} \quad (9)$$

with the corresponding boundary condition $\Gamma(x,|x|)=1$. The dependence of the kernel Γ on the relative times x follows from the differential equation

$$\left(-\frac{d^2}{dx^2}-\frac{\lambda/4\pi^2}{x^2+1}\right)\ \gamma_m(x)=-\frac{\omega_m^2}{4}\ \gamma^m(x). \quad (10)$$

For large λ the dominant part of the potential in Eq. (10) is from *small* relative times x resulting into a harmonic equation [12]

$$\left(-\frac{d^2}{dx^2}+\frac{1}{2}(\lambda/4\pi^2)x^2\right)\gamma_m(x)=-\frac{1}{4}(\omega_m^2-\lambda/\pi^2)\ \ \gamma_m(x). \quad (11)$$

This shows that the sum of the ladders grow exponentially. At large times $\mathcal{T}$, the kernel is dominated by the lowest harmonic mode of Eq. (11). For large times $\mathcal{S}\approx T$ that is small x and large y

$$\Gamma(x,y)\approx\mathbf{C}_0\ \ e^{-\sqrt{\lambda}\ x^2/4\pi}\ \ e^{\sqrt{\lambda}\ y/2\pi}. \quad (12)$$

From Eq. (6) it follows that in the strong coupling limit the ladder generated potential is

$$V_{\rm lad}(L)=-\frac{\sqrt{\lambda}/\pi}{L} \quad (13)$$

which has the same parametric form as the one derived from the AdS-CFT correspondence (1) except for the overall coefficient. Note that the difference is not so large, since $1/\pi=0.318$ is larger than the exact value 0.228 by about 1/3. So additional screening, left out to higher order diagrams, is needed to get it right.

B. Higher order diagrams and a "quasistring" regime

The results of Refs. [12] discussed above indicate that summing ladders get some vacuum physics but *not all* since the overall coefficient is not reproduced exactly. The same conclusion follows from the fact that the expectation values of Wilson lines are gauge invariant, while the ladder diagrams are not. Therefore, some non-ladder diagrams must be equally important and should be included.

Before we discuss any higher order diagrams, let us summarize what we have learned about the ladder resummation which are worth stressing. For that it is convenient to return to the integral form of the BS equation (5) and note that the inclusion of the kernel effectively forces the consecutive time steps between emission or absorption moments to be of the following duration:[1]

[1]The time ordering of interaction points along each line, reflecting on the non-Abelian character of the charges at large number of colors is important here.

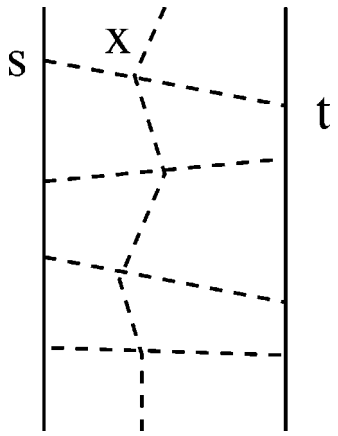

FIG. 3. Examples of higher-order diagrams with an extra scalar or gluon connecting the ladder rungs.

$$\delta s \approx \delta t \approx L/\lambda^{1/4}. \tag{14}$$

The overall number of time steps is huge and of the order of $N \approx \lambda^{1/4}\,\mathcal{T}/L$ as can be seen by the change of variables $(s,t)\rightarrow(x,y)$ in the Bethe-Salpeter equation. In the strong coupling regime the time steps are much shorter than in weak coupling. This implies that the speed of propagation of virtual quanta is forced to be parametrically *larger* than the speed of light,[2] with $v \approx \lambda^{1/4} \gg 1$. Thus it is the limitation on these two times which provides the reduction (or screening) factor $1/\sqrt{\lambda}$ in Coulomb's law for non-Abelian gauge theories at strong coupling.

Let us now look at higher order diagrams, e.g., Fig. 3 containing extra scalar or gluon line connecting the ladder rungs. Such diagrams can be resummed by a modified Bethe-Salpeter equation, for the function $\Gamma(s,t,\mathbf{x})$ where the last new argument is the 4D position of the new quantum on the rung. The RHS of the new Bethe-Salpeter equation has a modified kernel, so the last term in Eq. (5) now reads

$$\lambda^2 \int ds dt d\mathbf{y} \Delta(\mathbf{s}-\mathbf{y})\Delta(\mathbf{y}-\mathbf{t})\Delta(\mathbf{x}-\mathbf{y})\Gamma(s,t,\mathbf{y}), \tag{15}$$

with $\mathbf{s}=(s,\mathbf{0})$ and $\mathbf{t}=(t,\mathbf{L})$. As before, the integral equation can be transformed into a Schrödinger-like diffusion equation with a potential defined by this kernel. Furthermore, in strong coupling one can expand the denominators putting the small displacements in the numerator. This result in now a Coulomb plus oscillator potential of the type

$$V \approx \lambda \left(\frac{1}{(\mathbf{y}-\mathbf{x})^2} + \frac{\mathbf{C}}{L^2} + \frac{\mathbf{C}_{\mu\nu}}{L^4}\,\mathbf{y}_\mu \mathbf{y}_\nu \right), \tag{16}$$

where the 4D Coulomb[3] corresponds to the vertical propagator, from the old $(\mathbf{y})$ to the new $(\mathbf{x})$ position of the extra zig-zag quantum in Fig. 3. Again, the resulting Schrödinger-like equation can be solved and the lower level identified. Because of the large coefficient $\lambda \gg 1$ the transverse steps would be as small as the time steps, namely,

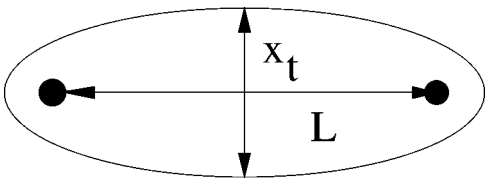

FIG. 4. Distribution of the interaction vertices in space. The black circles are static charges.

$$\delta \mathbf{x}_t \sim L/\lambda^{1/4}. \tag{17}$$

Thus the $d^4\mathbf{x}$ integration yields a suppression factor of $(1/\lambda^{1/4})^4 \approx 1/\lambda$. Since the $dsdt$ integrations bring about a suppression $(1/\lambda^{1/4})^2 \approx 1/\sqrt{\lambda}$, it follows that Eq. (15) is of the order $\sqrt{\lambda}$. This is precisely *the same order* as the modified potential discussed in the previous subsection. So, such higher order diagrams are neither larger nor smaller than the ladder ones we discussed earlier.

Needless to say, that one can also consider more elaborate ladder-type sequences containing more than one extra quantum, with extra power of the coupling again compensated by restrictions from extra $d\mathbf{y}$ integrations. Furthermore, since the number of quanta is not conserved — they can be absorbed by Wilson lines — one should consider the extended set of *coupled* BS equations for any number of quanta. We will not attempt to write them down explicitly here. However, what we retain from this discussion, is that all extra quanta prefer to be in an ellipsoidal region of space as shown in Fig. 4. The transverse sizes $\mathbf{x}_t \approx \delta t \approx L/\lambda^{1/4}$.

In QCD and other confining theories we known that gluons make a string between two charges with a constant width and tension: attempts to derive it from resummed diagrams continue. In CFT under consideration the width in transverse direction must be proportional to L since the conformal symmetry prohibits any other dimensional scale to be developed. Still, in strong coupling the ellipsoid is very elongated $\mathbf{x}_t \approx L/\lambda^{1/4} \ll L$: this is what we meant by a ''quasistring'' regime in the title of this subsection.

In principle, the calculation based on the AdS-CFT correpondence not only yields the potential (1) but also the local distribution of the energy density in space as well. It would be interesting to investigate whether one can elevate the whole discussion from the global potential to the differential distributions, in the form of resummed diagrams with extra quanta.

III. DEEPLY BOUND STATES AT FINITE *T*

A. Bound states in the quark-gluon plasma phase of QCD

Before we discuss the occurence of bound states in the Coulomb phase of CFT, we recall a similar occurence in nonsupersymmetric theories such as QCD in the deconfined or Coulomb phase. At high temperature the color charge in non-Abelian gauge theories is deconfined but *screened*

[2]Since no information is carried over, there is no problem with causality.

[3]In 4D the quadratic potential does not create solutions falling to the center.

(rather than antiscreened as in the perturbative vacuum) [13]. The resulting phase is called a quark gluon plasma (QGP). Analytical and numerical (lattice) calculations concur on the fact that at very high temperature, the fundamental fields (quarks and gluons for QCD) in the QGP behave as free propagating quasiparticles.[4]

Although the perturbative series of the bulk thermodynamics, such as the free energy, the pressure, the entropy, are found to be badly divergent at T comparable to T_c, it is somehow hoped that some sort of resummation will make the weak-coupling quasiparticle picture work, as the electric screening would keep the effective coupling weak for $T > T_c$. The very first suggestions for the QGP signal were a disappearance of familiar hadronic peaks such as ρ, ω, ϕ mesons in the dilepton spectra [18]. Even small-size deeply-bound $\bar{c}c$ states such as $\eta_c, J/\psi$, were expected to melt in the QGP at $T > T_c$ [19,20].

This picture has been challenged in our preceding work [1], where we argued that in the window of temperatures $T \approx (1\text{-}3)T_c$ the effective coupling can run up to large values. For $\alpha_s \approx 1$ we have $\lambda = g^2 N_c \approx 40$, before it is cut off by screening. We had shown that this leads to (loosely) bound states of $\bar{c}c, \bar{q}q, gg, qg, \bar{q}g$ s-wave states, explaining recent lattice observations [21,22].

This window of temperatures is very important, as it is the only one which is experimentally accessible, e.g., by RHIC experiments in Brookhaven National Laboratory. We argued in our recent work [1] that the existence of such weakly bound states leads to large scattering lengths and cross sections of quasiparticle rescattering, radically changing the kinetic properties of the QGP. This observation is crucial for understanding why in experiments, such as those at the Relativistic Heavy Ion Collider, the QGP behaves like a near-perfect liquid and displays prompt collective hydrodynamical behavior.

B. Heavy-light composites and related correlators

In view of this recent development in QCD, we are led to ask whether strongly coupled CFT in its Coulomb phase for all couplings (no phase transition) allow for hadronic bound states, and what role if any those may play at finite temperature. To keep the presentation simple, we will exemplify our method by analyzing the simplest ''heavy-light meson'' formed of a pair of an (auxiliary) static and light fermions. As noted by one of us [23], such states are the ''hydrogen atoms'' of hadronic physics, allowing us to start with a single-body problem instead of a many-body one.

We focus on a static (infinitely heavy) particle accompanied by a light one with opposite (adjoint) color. In CFT the light particle can be either a scalar, a gluino or a gluon.[5] In general, one can address the problem by considering the correlator of a quark (antiquark) field with a time-like (heavy) Wilson line [23] in Euclidean space,

$$\mathbf{C}(T) = \langle \mathrm{Tr}(\Psi^+(T,\mathbf{0})\mathbf{W}(T,0)\Psi(0,\mathbf{0})\mathbf{W}^+(T,\mathbf{0})) \rangle, \quad (18)$$

with Ψ the massless adjoint antiquark of the SYM theory and

$$\mathbf{W}(T,\mathbf{0}) = \exp\left(-ig \int_0^T dt \ \ \dot{x}(t) \cdot A(t,\mathbf{0}) \right) \quad (19)$$

the infinitely heavy adjoint quark. In the string-theory context this correlator would correspond to an open string. It is possible to evaluate Eq. (18) using the AdS-CFT correspondence at finite temperature, i.e., in the presence of a black hole. On the other hand, the correlator can be directly calculated by solving the Green function equation with a modified (strong coupling and screemed) Coulomb potential. If the two methods yield the same result, this would vindicate our physical description based on a near-instantaneous potential.

Here instead, we note that the large Euclidean time behavior of the correlation function (18) is controlled by the lowest heavy-light fermion bound state, i.e., $\mathbf{C}(T) \approx e^{-ET}$. The bound states are solution to the relativistic Dirac (Klein-Gordon, Yang-Mills) equation for gluinos (scalars, gluons) with a screened Coulomb potential to be derived below [see Eq. (29) below]. It is important to note that at finite temperature all quasiparticles develop a mass (as well as a width through collisional broadening) which sets the scale for the bound state problem even for the unscreened Coulomb potential. In CFT the thermal masses are generically of the form

$$m(T,\lambda) \approx T\lambda^{\alpha} \quad (20)$$

with some power α. Below we assume $\alpha = 1/2$ in strong coupling, based on the modified Coulomb law and Debye length $1/T$. (The mass scale then happens to be exactly like in weak coupling.)

C. Relativistic (WKB) spectrum for the Coulomb potential

The simplest bound state problem in our case is that of a gluino in the presence of an infinitly heavy source with compensating color charge. The latter acts as an overall attractive Coulomb potential V (the effects of screening will be discussed below). In strong coupling V acts on the accompanying relativistic gluino quasi-instantaneously. For a spherically symmetric potential, the Schrödinger-like equation is radial and reads

$$-\frac{d^2}{dr^2}\chi_l = \left[(E-V)^2 - m^2 - \frac{\tilde{l}^2}{r^2} \right] \chi_l \quad (21)$$

with the gluino wave function $\phi = Y_{lm}\chi_l(r)/r$ and the orbital quantum number $\tilde{l}^2 = l(l+1)$. For a semiclassical analysis, we will use the Langer prescription $l(l+1) \to (l+1/2)^2$, which is known to yield semiclassically stable S states. For a Coulomb-like potential, Eq. (21) is exactly solvable in terms of hypergeometric functions, much like the nonrelativistic

[4]Modulo color-magnetic effects that are known to be nonperturbative at all temperatures [14].

[5]The spin of the infinitely heavy charge is of course of no relevance and can be arbitrary.

problem for a hydrogen atom. It is however physically more transparent to use a semiclassical treatment in the manner of Bohr.

Identifying the LHS of Eq. (21) with the radial momentum squared, one can readily construct the necessary ingredients of WKB. Those are the turning points, roots of the RHS of Eq. (21), which for the generic Coulomb potential $V=-C/r$ are

$$r_{1,2}=\frac{1}{E^2-m^2}(EC\pm\sqrt{m^2C^2+\tilde{l}^{\,2}(E^2-m^2)}). \qquad (22)$$

It is important that r is a radial variable, so that both solutions in Eq. (22) are *positive*, for otherwise we are dealing with either a scattering state returning to large r, or an inward falling state with a wave towards small r. For small coupling C the positivity condition is always satisfied, while for large C the positivity condition is only satisfied for orbital motion with $\hat{l}\approx(\sqrt{\lambda}+1/\sqrt{\lambda})$.

Using the Bohr-Sommerfeld quantization one introduces the radial quantum number and gets[6]

$$\int_{r1}^{r2}p_r dr=\pi(n+1/2)$$

$$=\pi\left(1-\frac{E_{nl}}{\sqrt{E_{nl}^2-m^2}}\frac{C}{\sqrt{\tilde{l}^2-C^2}}\right) \qquad (23)$$

from which the quantized levels are

$$E_{nl}=\pm m\left[1+\left(\frac{C}{n+1/2+\sqrt{\tilde{l}^2-C^2}}\right)^2\right]^{-1/2}. \qquad (24)$$

In weak coupling $C=g^2N=\lambda$ is small and the bound states energies are close to $\pm m$. Specifically[7]

$$E_{nl}\pm m\approx-\frac{C^2m}{2(n+l+1)^2}, \qquad (25)$$

which is the known Balmer formula. In the (opposite) strong coupling limit the coefficient is large $C=(4\pi^2/\Gamma(1/4)^4)\sqrt{\lambda}\gg 1$. Unless the square root gets balanced by a sufficiently large angular momentum, the quantized energies are imaginary. This does not happen for $n,\sqrt{\tilde{l}^{\,2}-C^2}\approx\lambda^0$ and $C\approx\sqrt{\lambda}$, which are also the conditions for which both roots in Eq. (22) are positive. In this regime, one may ignore the 1 in Eq. (24) and obtain the *equidistant* spectrum

$$E_{nl}\approx\frac{m}{C}[(n+1/2)+((l+1/2)^2-C^2)^{1/2}]. \qquad (26)$$

Since the mass is related to the thermal loop with $m\approx\sqrt{\lambda}$, the ratio $m/C\approx T\lambda^0$ is proportional to temperature but *independent* of the coupling constant.

More details on the WKB spectrum are shown in Fig. 5 for different values of the orbital quantum number l (a) and radial quantum number n (b). All lines end when the Coulomb attraction is able to overcome the centrifugal repulsion.

In summary we have put forward an explanation for the occurence of a tower of light composite states with energies (masses) that are independent of the strong coupling λ. The composites are strongly bound Coulomb states which occur relativistically due to a balance between the strong Coulomb attraction and the repulsive centrifugation in an l state. Only the states with $(l+1/2)\geqslant\sqrt{\lambda}/\pi$ bind, resulting into an equidistant WKB spectrum. The critical coupling for S states is

$$g_c=\frac{\pi}{\sqrt{N_c}}\ \text{ or }\ \lambda_c=\pi^2. \qquad (27)$$

Note that the orbital states with $l\approx\sqrt{\lambda}$ are either bound (real) or unbound (complex). The complex states correspond to the case were the light relativistic particle collapses onto the heavy source due to the large Coulomb attraction overcoming centrifugation. At $T=0$ these states may pair condense in the form of neutral dipoles at the origin of the large dielectric constant $\epsilon\approx\sqrt{\lambda}$.

D. Effects of screening

In so far we have ignored in the WKB spectrum the effects of screening on the Coulomb potential. To assess that, we will show below that in strong coupling the screened Coulomb potential between scalars is mostly mediated by the electric gluons, leading to

$$V(\mathbf{x})=-\frac{C}{|\mathbf{x}|}\ \mathbf{F}_E(T\mathbf{x}) \qquad (28)$$

with

$$\mathbf{F}_E(T\mathbf{x})=\frac{(\pi T|\mathbf{x}|)}{|\mathrm{sh}(\pi T|\mathbf{x}|)|}. \qquad (29)$$

In strong coupling the effective screening length is $1/(\pi T)$ independent of the coupling constant. This result is remarkably in agreement with lattice QCD simulations in the (1–3) T_c window. The derivation of Eq. (29) using screened ladders graph with $C=\sqrt{\lambda}/2\pi$ is given below. Note that at $T=0$ Eq. (28) reduces to the unscreened Coulomb potential.

How would the screened potential (28) affect our WKB spectrum? The answer is only marginal. Indeed, if we insert Eq. (24) back to the expressions for the radial turning points (22), we find that the largest turning point occurs for

[6]In order to avoid confusion: what we call n is not the principal quantum number but just a radial one. So there are no relation or limits on it for any l.

[7]The fact that only the combination $n+l$ appears, i.e., principle quantum number, is a consequence of the known Coulomb degeneracy. This is no longer the case in the relativistic case.

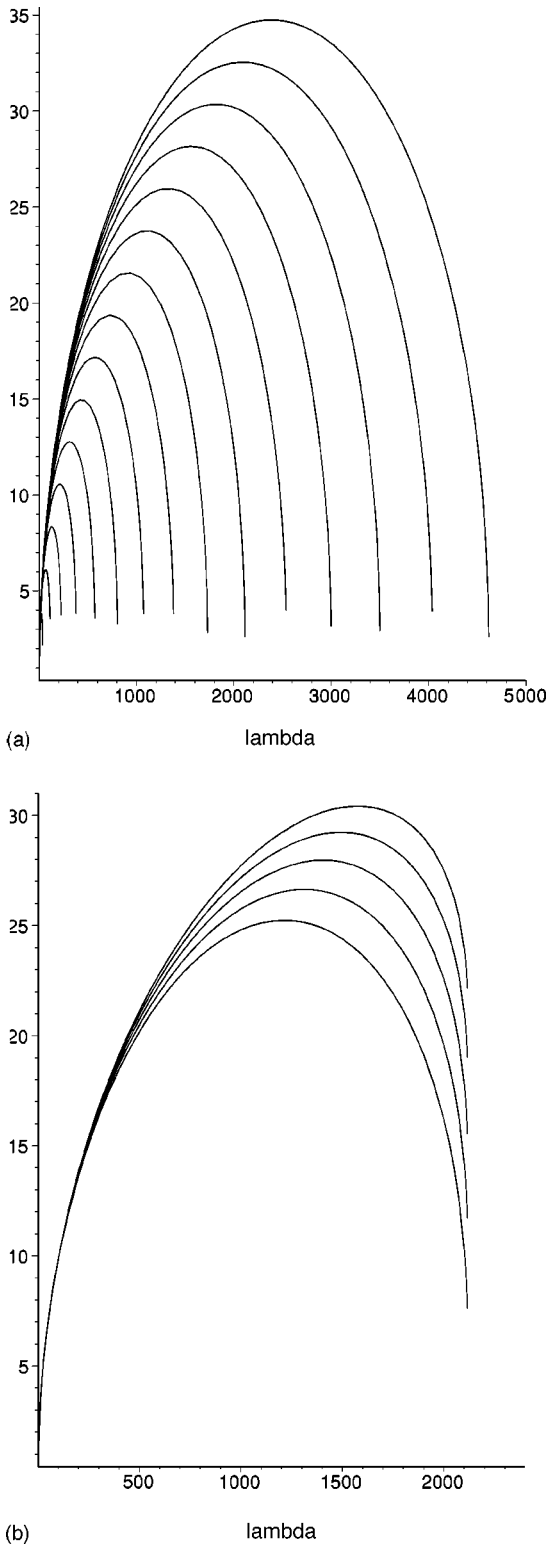

FIG. 5. The WKB spectrum versus 't Hooft coupling constant λ. (a) Levels with fixed $n=0$ and $l=1\ldots15$; (b) levels with fixed $l=10$ and $n=0\ldots5$.

$r_2 \approx 1/T$ which is comparable to the screening radius following from Eq. (28). We note in passing, that the size of the Coulomb bound state in strong coupling is very small and of order $1/(\sqrt{\lambda}T)$.

E. More details on the bound states

The semiclassical arguments developed above were curtailed to scalars. How would they work for gluons and gluinos? To answer qualitatively this question, we recall that in a weakly coupled plasma, the number and nature of the gluons and gluinos is different from free massless waves of the free theory. For instance the gluons carry 2 polarizations in free space, while in the plasma a third one appears, the plasmon [13]. Also the fermions develop different excitation modes depending whether chirality and helicity are the same or opposite,[8] see e.g. [15] for a general discussion and weak coupling results. In the latter case the mode is called a plasmino.

If the dispersion laws for gluons and gluinos were known, the effective equation of motion suitable for the discussion of the bound state problem can be obtained by standard substitution of the covariant derivatives in the place of momentum and energy. The electric effective potential would then go together with the energy. For two gluinos, it is

$$V_{qQ}(\mathbf{x}) = -\frac{C}{|\mathbf{x}|}\gamma_4 \mathbf{F}_E(T\mathbf{x}). \tag{30}$$

Unfortunately, we do *not* know the pertinent dispersion laws for strongly coupled CFT. We only know from lattice studies [16] that in the window $T=(1-3)T_c$ for which the QCD plasma is likely in a moderatly strong Coulomb phase, the dispersion law for both quarks and gluons is of the canonical type $\omega^2 = k^2 + m_F^2$. For fermions, m_F is not the usual (chiral violating) mass term, but rather a thermal chiral mass. This dispersion relation can be incorporated in a linear Dirac equation through a chiral mass of the form $\gamma_4\, m_F^2/E$, resulting in the following equation:

$$\left(\left(E - \frac{m_F^2}{E}\right) + i\alpha\cdot\nabla + \frac{\sqrt{\lambda}/2\pi}{x}\,\mathbf{F}_E(xT)\right) q(\mathbf{x}) = 0. \tag{31}$$

The above WKB analysis can be carried out for Eq. (31) as well, with similar conclusions as the ones reached for the relativistic scalars.

IV. THERMODYNAMICS AND KINETICS AT STRONG COUPLING

A. AdS-CFT results

The CFT thermodynamics at strong coupling has been studied by a number of authors [8]. It was found that the free energy in this limit is

$$\mathbf{F}(T,N_c,\lambda) = ((3/4) + O(1/\lambda^{3/2}))\mathbf{F}(T,N_c,0), \tag{32}$$

where $\mathbf{F}(T,N_c,0) \approx N_c^2 T$ is the free (zero coupling) result, analogous to the Stephan-Boltzmann result for blackbody radiation. The kinetics of the finite-T CFT at strong coupling was recently investigated also using the AdS-CFT correspon-

[8]We ignore the U(1) axial anomaly and instantons, and consider the L,R chiralities to be absolutely conserved quantum numbers.

dence [9]. In particular, the viscosity of strongly coupled matter was found to be unusually small, leading to a rather good liquid with hydrodynamical behavior even at small spatial scales. In particular, the sound attenuation length (analogous to the mean free path) was found to be [9]

$$L^S_{sound}=\frac{4}{3}\frac{\eta}{sT}=\frac{1}{3\pi T}, \tag{33}$$

where η,s are the viscosity coefficient and entropy density, respectively. This length is much *shorter* than in the weak coupling

$$L^W_{sound}=\frac{\text{const}}{Tg^4\ln(1/g)}\gg\frac{1}{T}. \tag{34}$$

As we have mentioned in the Introduction, such results are rather puzzling dynamically from the gauge-theory standpoint. Normally all kinetic quantities are related with scattering cross sections, and the absence of *any* coupling is *a priori* implausible physically. In general, thermodynamical quantities count degrees of freedoms and one may think that the coupling constant may indeed be absent. However, the effective masses of the quasiparticles and all pairwise interactions are still proportional to $\sqrt{\lambda}$ and in general λ^α with $\alpha>0$. If so, the quasiparticle contributions to the statistical sum should be exponentially small at strong coupling, of the order of $e^{-\lambda^\alpha}\ll 1$, and one will have to conclude that some other degrees of freedom are at play.

Indeed there are new degrees of freedom at play in the strong coupling regime of the thermal Coulomb phase. As we have shown above, for large λ there are light (deeply bound) binary composites, with masses of order T irrespective of how strong is λ. The composites are almost pointlike with thermal sizes of the order of $1/T$, which readily explains the liquid-like kinetic behavior. The thermal Coulomb phase is a liquid of such composites. The composites are light and should dominate the long-distance behavior of all the finite temperature Euclidean correlators.

B. Gauge theory: Quantitatively

We start by explaining the leading contribution (32) from the gauge theory point as a liquid of composites. The factor of N_c^2 in front of the free energy and the viscosity for instance, follows from the fact that *all* our composites are in the adjoint representation. Indeed, for fundamental charges the composites are mesonlike (color neutral) with all color factors absorbed in the coupling constant. For adjoint charges, there is in addition *two* spectator charges[9] that do not participate into the binding. The Coulomb phase is not confining. Thus the number of light and Coulomb bound composites is N_c^2.

[9]For example, a composite can be initially made of blue-red and red-green colors, with red rapidly changing inside the ladder. One can view it as two extra vertical lines added to Fig. 2(a).

The astute reader may raise the question that by now our arguments are totally circular: we have started with N_c^2 massless relativistic states and we have returned to N_c^2 light composites. So what is the big deal? Well, the big deal is that we are in strong coupling, and in fact the degrees of freedom completly reorganized themselves in composites, for otherwise they become infinitly heavy thermally and decouple. This is how Coulomb's law negotiates its deeds in a system with very large charges.

The composites carry large angular momentum in strong coupling, i.e., $l\approx\sqrt{\lambda}$. Their weight contribution to the partition function is of the order of

$$\int_{l_{min}}^{l_{max}} dl^2=l^2_{max}-l^2_{min}\approx\lambda^0, \tag{35}$$

which is independent of λ, since the WKB orbits are stable only for $l\approx(\sqrt{\lambda}+1/\sqrt{\lambda})$. The ensuing thermodynamical sum over the radial quantum number n is independent of λ, leading to a free energy $\mathbf{F}=-(\mathbf{C}\pi^2/6)N_c^2\,T$ in agreement with Eq. (32). For weak coupling $\mathbf{C}=1$ while for strong coupling $\mathbf{C}=3/4$.

The overall coefficient in the N_c^2 part of the free energy in strong coupling is harder to obtain from the gauge theory side although the WKB spectrum could be used to assess it. A simple example on how this arises in strong coupling and at large number of colors was shown in [17]. Alternatively, if we refer to the coupling-valued coefficient by $\mathbf{C}(\lambda)$ and assume it to be an analytic function in the complex λ-plane modulo singularities, then $(\lambda>0)$

$$\mathbf{C}(\lambda)=\mathbf{C}(0)+\frac{\lambda}{\pi}\int_{+0}^{\infty}d\lambda'\,\frac{\text{Im}\,\mathbf{C}(-\lambda')}{\lambda'(\lambda'+\lambda)}. \tag{36}$$

If the imaginary part along the negative real axis is bounded, the RHS is λ independent in strong coupling. To proceed further requires a better understanding of the singularity structure of the free energy in the complex plane, e.g., the Dyson singularity in weak coupling which suggests $\text{Im}\,\mathbf{C}(-\lambda)\approx e^{-1/\lambda^\alpha}$ with typically $\alpha=1$. This point will be pursued elsewhere.

V. SCREENING AT FINITE TEMPERATURE: PRELIMINARIES

At finite temperature and in Euclidean space, the Wilson loops can be divided into electric (E) and magnetic (M) ones. The electric Wilson loop is sensitive to Coulomb's law between static charges, while the magnetic Wilson loop is sensitive to Lenz's law between two running currents. In the Euclidean vacuum $O(4)$ symmetry rotates one to the other, and we expect the same modified Coulomb's law (38) in CFT. In non-CFT theories such as QCD they are both confining.

The usual definition of the ''screened potential'' implies that at $r\to\infty$ the potential vanishes. However, there is a residual *negative* constant mass renormalization at finite T, due to the self-interaction of a static charge with its thermal

cloud. In weak coupling it is of the order of $\lambda^{3/2}T$ [13] using Debye's argument, and in strong coupling it is of the order of $\sqrt{\lambda}T$ [4]. This *negative* correction to the mass of a static charge should not be confused with the *positive* effective mass of quasiparticles which is of order $\sqrt{\lambda}T$ as well.

A. Magnetic screening and AdS-CFT

At nonzero temperature T Euclidean space is a cylinder of radius $\beta=1/T$, and the $O(4)$ symmetry is reduced to $O(3)$ symmetry with no a priori relationship between the electric and magnetic Wilson loops. In non-CFT theories such as QCD and in weak coupling, the electric charges are Debye screened while the magnetic charges are not [13]. Weak-coupling nonperturbative effects related to spatial confinement in high temperature 3D YM theory, are believed to generate a magnetic mass of order λT [14]. Several lattice calculations support this idea, leading a nonzero spatial string tension of order $\lambda^2 T^2$.

What happens at strong coupling? Our first new observation in CFT theories, is that at strong coupling the AdS-CFT correspondence yields magnetic screening which is the *same* as the electric screening observed in [4]. Thus for large spatial separation

$$V_M(\beta,L)=V_E(\beta,L)=\frac{\sqrt{\lambda}}{L}f(\beta/L), \tag{37}$$

where $f(\beta/L)$ was evaluated in [4] for electric Wilson loops. The simple way to see this is to recall that the modified Coulomb's law for the electric Wilson loop follows from the *pending* string in the 5th direction as shown in Fig. 2. This phenomenon is unmodified for spatial Wilson loops, whereby the minimal surface is still of the same nature. Note that the temperature in this case is given by a suitable choice of the radius of the black hole. At strong coupling the electric and magnetic scales are the same, since there is no apparent spatial confinement in high temperature CFT.

B. Naive (unscreened) ladders at finite T

Naively, the first step toward the calculation of the potential between charges at finite temperature is the same resummation of the ladder diagrams via Bethe-Salpeter equation, but with thermal propagators for gluons or scalars. Let us see, for pedagogical reasons, what this procedure will produce. We can apparently have either electric or magnetic ladders, thus the expression becomes

$$V_{E,M}(L)=-\lim_{\mathcal{T}\to+\infty}\frac{1}{\mathcal{T}}\ln\Gamma_{E,M}(\mathcal{T},\mathcal{T}). \tag{38}$$

The electric kernel is generated through

$$\frac{\partial^2\Gamma_E}{\partial\mathcal{S}\ \partial\mathcal{T}}=\sum_{n=-\infty}^{\infty}\ \frac{\lambda/4\pi^2}{(n\beta)^2+(\mathcal{S}-T+n\beta/L)^2+L^2}\Gamma_E(\mathcal{S},T), \tag{39}$$

and the magnetic kernel through

$$\frac{\partial^2\Gamma_M}{\partial\mathcal{S}\ \partial\mathcal{T}}=\sum_{n=-\infty}^{\infty}\ \frac{\lambda/4\pi^2}{(n\beta)^2+(\mathcal{S}-T)^2+L^2}\Gamma_M(\mathcal{S},T). \tag{40}$$

Both kernels are subject to the boundary conditions

$$\Gamma_{E,M}(\mathcal{S},0)=\Gamma_{E,M}(0,\mathcal{T})=1. \tag{41}$$

As in the zero temperature case [12] the equations are separable in $x=(\mathcal{S}-T)/L$ and $y=(\mathcal{S}+T)/L$ with the appropriate boundary conditions. The temporal and spatial kernels separate

$$\Gamma_{E,M}(x,y)=\sum_m\ \mathbf{C}_m\gamma^m_{E,M}(x)e^{\omega^m_{E,S}y/2}, \tag{42}$$

with the **C**'s fixed by the boundary conditions, and the γ's obeying the one-dimensional Schrödinger equation in a periodic potential, which is

$$\left(-\frac{d^2}{dx^2}-\sum_{n=-\infty}^{\infty}\frac{\lambda/4\pi^2}{(x+n\beta/L)^2+1}\right)\gamma^m_E(x)=-\frac{{\omega^m_E}^2}{4}\ \gamma^m_E(x) \tag{43}$$

for the temporal kernel and

$$\left(-\frac{d^2}{dx^2}-\sum_{n=-\infty}^{\infty}\ \frac{\lambda/4\pi^2}{(n\beta/L)^2+x^2+1}\right)\gamma^m_M(x)=-\frac{\omega^{m2}_M}{4}\gamma^m_M(x) \tag{44}$$

for the spatial kernel. The sum of the ladder diagrams grows exponentially: $\Gamma(0,y)\approx e^{\omega_0 y/2}=e^{\omega_0 T/L}$. From Eq. (38) it follows that the screening at finite temperature is given by the ground state eigenvalue $\alpha_{E,M}=\omega^0_{E,M}(\lambda,\beta/L)$.

In the strong coupling limit, the potential is peaked at $x=0$ modulo β. Although the solutions to the periodic problem yields in general a band structure, for $\lambda\gg1$ the ground state is just a particle trapped at $x=0$. The ground state energy follows from the harmonic approximation much like at zero temperature. The result for the electric screening is

$$\alpha_E=\frac{\sqrt{\lambda}}{\pi}\sqrt{\Sigma_1}-\sqrt{\frac{\Sigma_2}{2\Sigma_1}}+\mathcal{O}\left(\frac{1}{\sqrt{\lambda}}\right), \tag{45}$$

with

$$\Sigma_1=\sum_n \frac{1}{(n\beta/L)^2+1}=(\pi\ L/\beta)\coth(\pi L/\beta),$$

$$\Sigma_2=\sum_n \frac{1-(n\beta/L)^2}{((n\beta/L)^2+1)^3}$$
$$=-\frac{1}{2}(\pi L/\beta)^3\coth(\pi L/\beta)(1-\coth^2(\pi L/\beta))$$
$$+\frac{1}{4}\coth(\pi L/\beta)-\frac{1}{4}(\pi L/\beta)^2(1-\coth^2(\pi L/\beta)). \tag{46}$$

For the magnetic screening, the result is

$$\alpha_M=\frac{\sqrt{\lambda}}{\pi}\sqrt{\Sigma_1}-\sqrt{\frac{\Sigma_3}{2\Sigma_1}}+\mathcal{O}\left(\frac{1}{\sqrt{\lambda}}\right), \tag{47}$$

with

$$\Sigma_3=\sum_n \frac{1}{((n\beta/L)^2+1)^2}$$
$$=-\frac{1}{2}(\pi L/\beta)^2(1-\coth^2(\pi L/\beta))$$
$$+\frac{1}{2}(\pi L/\beta)\coth(\pi L/\beta). \tag{48}$$

In the strong coupling and to leading order, the planar resummations yield the same screening for the electric and magnetic Wilson loops,

$$\alpha_E\approx\alpha_M\approx\frac{\sqrt{\lambda}}{\pi}\left(1+2\sum_{n=1}^{\infty}\frac{1}{(n\beta/L)^2+1}\right), \tag{49}$$

where we have explicitly separated the thermal effects.

The result (49) appears to show that in strong coupling the potential is *stronger* at nonzero T than in vacuum. This agrees with strong coupling Debye screening calculations [4]. It may appear that it contradicts the fact that the screened potential should vanish at large r. The paradox is explained by the presence of a negative mass renormalization constant (static-charge interacting with its Debye cloud) as mentioned at the beginning of this section.

VI. SCREENED LADDERS AT FINITE T

The static charges wich interactions we study are not part of the $\mathcal{N}=4$ YM theory, so we are free to give them any interactions we want. So far we have followed the standard notations, in which the scalar and gluon exchanges are equal for $\bar{q}q$ and cancel for qq pairs. In this case the linear divergences cancel as well. However in-matter screening at finite T is different for scalars and gluons, so it is pertinent to discuss the screening sequentially.

A. Screened scalar ladders

The scalar polarization is simpler. In the lowest order it is given by a well known bubble diagram, leading to a momentum-independent polarization operator $m_D^2\approx\lambda T^2$. Its insertions induce a potential between two charges, in Euclidean space after analytical continuation with Matsubara periodicity:

$$\Delta(t,\mathbf{x})=iT\sum_n \int \frac{d\mathbf{k}}{(2\pi)^3}\frac{e^{-i\omega_n t+i\mathbf{k}\cdot\mathbf{x}}}{K^2+\Pi_{00}}, \tag{50}$$

where $K^2=\omega_n^2+k^2$. The zero mode $n=0$ contribution is a standard screened potential

$$\frac{iT}{4\pi x}e^{-m_D x}$$

and is therefore exponentially suppressed in strong coupling.

In strong coupling, even static charges communicate via high-frequency quanta (short times) so we now consider the nonzero mode contributions in Eq. (59). Performing the momentum integral yields

$$\frac{iT}{2\pi x}\sum_{n=1}\cos(\omega_n t)\frac{\omega_n^2}{\omega_n^2+M_D^2}e^{-\omega_n^2 x/\sqrt{\omega_n^2+m_D^2}}.$$

For large λ the Debye mass $m_D\gg\omega_n$, and the screened scalar propagator can be further simplified

$$\Delta(t,\mathbf{x})\approx\frac{iT}{4\pi x}\left(e^{-m_D x}+2\sum_{n=1}^{\infty}\cos(\omega_n t)\frac{\omega_n^2}{m_D^2}\ e^{-\omega_n^2\ x/m_D}\right). \tag{51}$$

Substituting the sum over n by the integral, combining the cosine with the exponent and completing the square in the exponent, one finally finds that the nonstatic part of the induced scalar potential vanishes in the strong coupling as $1/\sqrt{m_D}\approx 1/\lambda^{1/4}$.

B. Screened electric ladders

We now consider exchanges of electric gluons. In covariant gauges, the electric propagator in Euclidean momentum space reads in general

$$\Delta_{00}(\omega,\mathbf{k})=\frac{1}{K^4}\left(\frac{k^4}{k^2-\Pi_{00}}+(1-\alpha)\ \omega^2\right), \tag{52}$$

where α is the gauge parameter and, as before, $K^2=\omega^2+k^2$. In configuration space the propagator is then

$$\Delta_{00}(t,\mathbf{x})=iT\sum_{n=-\infty}^{\infty}\int\frac{d\mathbf{k}}{(2\pi)^3}\,e^{-i\omega_n t+i\mathbf{k}\cdot\mathbf{x}}\,\Delta_{00}(\omega_n,\mathbf{k}). \tag{53}$$

In weak coupling we need only the static limit with $\omega_n=0$. Therefore the gauge-sensitive term disappears and the first term yields the familiar Debye form with $\Pi_{00}(0,\mathbf{k})\approx m_D^2$.

In strong coupling we need the opposite limit, in which the frequency is high with $\omega \approx \lambda^{1/4}/L \gg k \approx 1/L$. Now the (gauge dependent) longitudinal part contributes $\Delta_{00} \approx (1-\alpha)/\omega^2$. The 00 part depends on the polarization operator, which at high frequency has the generic form

$$\Pi_{00}(\omega,\mathbf{k}) \approx \lambda T^2 \frac{k^2}{\omega^2}. \tag{54}$$

This result is the same as the one derived from hard thermal loops although in the opposite limit $T \gg \omega$. Below we explain why this similarity is not fortuitous. Inserting Eq. (54) into Eq. (52) one finds that one power of k^2 can be canceled, and the first term becomes of order $(k^2/\omega^2)/(\omega^2+\omega_p^2)$, with the denominator capable of producing the plasmon pole. However, this term is clearly subleading as compared to the longitudinal one. This happens because it lacks the enhancement through ω^2 in the numerator.

Inserting the electric part (60) in Eq. (53) and performing the momentum integration yields

$$\Delta_{00}(t,\mathbf{x}) = \frac{iT}{4}\left(\frac{e^{-m_D x}}{\pi x} + 2\sum_{n\neq 0}^{\infty} \cos(\omega_n t) e^{-\omega_n t} \frac{\omega_n^2}{\omega_n^2+\omega_p^2} \times \left(\frac{1}{\pi x} + \frac{1}{2\pi\omega_n}((1-\alpha)(\omega_n^2+\omega_p^2)-\omega_n^2) \right) \right), \tag{55}$$

where the first and screened contribution arises from the zero mode and the second contribution arises from the nonzero modes in the high frequency (short time) regime $\omega \gg k$. In the strong coupling limit $\omega_D/T \approx \sqrt{\lambda} \gg 1$, Eq. (55) reduces to

$$\Delta_{00}(t,\mathbf{x}) = (1-\alpha)\frac{iT}{4\pi}\sum_{n=1}^{\infty} \cos(\omega_n t)\omega_n e^{-\omega_n x}, \tag{56}$$

which is controlled by the first Matsubara frequency at large distance. It is readily checked that for $t=0$

$$\Delta_{00}(0,\mathbf{x}) = (1-\alpha)\frac{ixT^2}{8\,\mathrm{sh}^2 \pi T x}, \tag{57}$$

which reduces to the free electric part of the covariant propagator at $T=0$. This part is the chief contribution to the screened electric ladders in the strong coupling. Indeed, a rerun of the previous Bethe-Salpeter resummation using Eq. (56) as the screened ladder shows that only the short time limit of Eq. (57) contributes as $\lambda \gg 1$. In particular, the electric potential between two Wilson lines with only adjoint A fields is

$$V_E(Tb,\alpha) = -\frac{\sqrt{\lambda}/\pi}{b}\mathbf{F}_E(bT,\alpha), \tag{58}$$

with

$$\mathbf{F}_E(bT,\alpha) = \sqrt{1-\alpha}\,\frac{\pi T x}{|\mathrm{sh}(\pi T x)|}, \tag{59}$$

which is seen to reduce to the $T=0$ result in Feynman gauge. As noted above, the result (59) yields a screening length of order $1/(\pi T)$ in strong coupling, which is *larger* than the $1/(\sqrt{\lambda}T)$ expected from weak coupling. Again, the strong coupling result is even consistent with current QCD lattice simulations which suggest that the Debye screened potential screens at about a distance of order $1/\pi T$.

Finally, the result (59) is gauge sensitive, and one may question the interpretation of our results. Of course the same criticism for summing the ordered ladders hold at $T=0$ as well. However, we expect our main observations in covariant gauge to hold for the reason that the results agree overall with results from the ADS-CFT correspondence both at $T=0$ and finite T for the electric sector. Retardation is best captured in covariant gauges, and that was seen as key in describing the screening at work in the ground state.

C. Hard thermal loops at short times

The effects of matter is more than the Bose enhancement. It is usually due to a genuine screening of the Coulomb interaction. How would this work at strong coupling? The answer would be in general hopeless, except for yet another important observation: The induced interaction occurs in our case over very *short* times. This means that we probe the thermalized but strongly coupled Coulomb phase over short periods of time, in which case the thermal distributions are left unchanged. As a result, the high frequency modes are screened at strong coupling in exactly the same way as they are in *weak* coupling at high temperature.

This is best seen using a first quantized analysis of screening in terms of transport arguments, whereby the only assumption needed to derive the hard thermal loops is that the thermal distribution be expandable into $f=f^0+f^1 \approx f^0$ for $f^1/f^0 \ll 1$ at short times. In Euclidean space (Matsubara frequencies) the hard thermal loops reduce to

$$\Pi_{00}(\omega,k) = -\omega_D^2\left(1-\frac{\omega}{2k}\ln\left|\frac{\omega+k}{\omega-k}\right|\right),$$

$$\Pi_{ii}(\omega,k) = \frac{\omega_D^2}{2}\left(\frac{\omega}{k}\ln\left|\frac{\omega+k}{\omega-k}\right|\right). \tag{60}$$

The zero Matsubara frequencies are electrically screened with $\Pi_{00}=-\omega_D^2$ and magnetically free with $\Pi_{ii}=0$. The situation is somehow reversed at high Matsubara frequencies with

$$\Pi_{00} \approx -\omega_p^2\frac{k^2}{\omega^2},$$

$$\Pi_T(\omega,k) \approx \omega_D^2. \tag{61}$$

The plasmon frequency is defined as $\omega_p^2=\omega_D^2/3$ with the Debye frequency $\omega_D=m_{G,\phi,F}$ for the gluons, scalars and quarks read respectively

$$m_G^2\approx m_F^2\approx m_\Phi^2\approx\lambda T^2. \tag{62}$$

The electric modes are free at high frequency, while the magnetic modes are Debye screened. This is just the opposite of what happens at low frequency. Still, *both* the dielectric constant and inverse magnetic permittivity vanish at large frequency. The thermal medium is transparent to high frequency electric and magnetic fields as it should.

D. Screened magnetic ladders

The real insertions (60) induce a new potential between two moving charges in Euclidean space after analytical continuation. In covariant gauge, the resummed magnetic propagator in Euclidean momentum space reads ($K^2=\omega^2+k^2$)

$$\Delta_{ij}(t,\mathbf{x})=(-\delta_{ij}+\nabla_i\nabla_j)iT\sum_n\int\frac{d\mathbf{k}}{(2\pi)^3}\frac{e^{-i\omega\ t+i\mathbf{k}\cdot\mathbf{x}}}{K^2+\Pi_T}$$
$$+\nabla_i\nabla_j iT\sum_n\int\frac{d\mathbf{k}}{(2\pi)^3}\frac{e^{-i\omega\ t+i\mathbf{k}\cdot\mathbf{x}}}{K^4}$$
$$\times\left(-\frac{\omega^2}{k^2+\Pi_{00}}+(1-\alpha)\right). \tag{63}$$

Performing the momentum integrations, taking the strong coupling limit $\lambda\gg 1$ and contracting the answer with the particle velocities $\mathbf{v}_{1,2}$ attached to the external Wilson lines yield

$$\mathbf{v}_{1i}\mathbf{v}_{2j}\Delta_{ij}=2\mathbf{v}_1\cdot\mathbf{v}_2\frac{iT}{4\pi\ x^3}$$
$$\times\left(-\frac{x^2}{2}\delta_{=0}+\frac{1}{m_M^2}\delta_{\neq 0}+\frac{1}{\omega_p^2}-\frac{1}{\omega_D^2}\right), \tag{64}$$

where we have inserted a magnetic mass $m_M/T\approx\lambda$ on the transverse magnetic zero mode. $\delta_{=0}$ is the contribution when the magnetic mass is zero (long range field), while $\delta_{\neq 0}$ is the contribution when the magnetic mass is inserted (short range field). Clearly, the magnetic contribution survives the strong coupling limit only in the absence of a magnetic mass. The contribution to the ladder resummation follows from the basic insertion

$$\frac{i\lambda}{2}\mathbf{v}_{1i}\mathbf{v}_{2j}\Delta_{ij}.$$

The screened magnetic ladders yield a magnetic potential that is different from the electric one derived above in coupling and range if a magnetic mass is present. In the absence of an induced magnetic mass, the electric and magnetic potentials exhibit a similar behavior in coupling, but are distinct in range. The magnetic potential still has infinite range, while the electric potential has a finite range of order $1/\pi T$ as we indicated above. The simple AdS-CFT argument provided earlier leads to the same electric and magnetic screening length. The understanding of this point from the gauge theory standpoint is worth pursuing.

VII. SUMMARY AND OUTLOOK

We have exploited the fact that $\mathcal{N}=4$ SYM theory is in a Coulomb phase at all couplings, to argue that in strong coupling (Maldacena regime) color charges only communicate over very short periods of time $t\approx L/\lambda^{1/4}$ for a fixed separation L. This physical observation is enough to show why ladderlike diagrams in the gauge theory reproduce the modified Coulomb's law obtained by the AdS-CFT correspondence using classical gravity. This class of diagrams is however not complete since the answer is gauge-sensitive. We have shown that the insertion of additional quanta along the ladder brings about extra factors of $\lambda\int d^4\mathbf{x}\approx\lambda^0$, leading to a quasistring geometry. In $\mathcal{N}=4$ SYM theory the quasistring has a transverse to a longitudinal ratio of order $(L/\lambda^{1/4})/L\ll 1$, but is not confining.

These observations are generic and suggest that in the gauge theory the modified Coulomb potential applies equally well to relativistic and nonrelativistic charges. Indeed, since the relativistic particles move with velocity $v\approx 1$, the color reordering encoded in the modified Coulomb potential goes even faster through a virtual quantum exchange with velocity $v\approx\lambda^{1/4}\gg 1$. *At strong coupling and/or large number of colors*, the charge is so large that color rerrangement is so prohibitive unless it is carried instantaneously. This is the only way Coulomb's law could budget its energy. The same observations extend to finite temperature where we have shown that the modified Coulomb potential acquires a screening length of the order of $1/T$ irrespective of how strong is the coupling. This observation seems to be consistent with current lattice simulation of nonconformal gauge theories in their moderatly strong Coulomb phase, e.g., QCD.

We have analyzed the effects of a (supercritical) Coulomb field on the motion of colored relativistic particles. Bound states form whenever the squared Coulomb potential balances the effects of centrifugation. In strong coupling the resulting bound state spectrum is oscillatorlike, in agreement with the tower of resonances observed using the AdS-CFT correspondence [10,11]. Rather unexpectedly, we have found that even though the trajectory of any particular Coulomb bound state depends critically on the coupling λ, their average density remains constant in the strong coupling domain. This finally leads to a *universal gas of composites* in strongly coupled CFT, a nice parallell with recent developments in QCD [1].

Clearly our work is only the first attempt in trying to understand from the gauge theory standpoint the intricate and surprising results obtained by the AdS-CFT correspondence both in vacuum and matter. In particular, our discussion of the spectroscopy of composites, Debye screening, thermodynamics and kinetics of matter were rather sketchy,

with only the qualitative trends emphasized. All of this can obviously be worked out with more details that go beyond the scope of the current presentation.

However, it is clear that the dynamical picture we have put forward from the gauge theory standpoint goes beyond the confines of supersymmetry or the conformal nature of the strongly coupled gauge theory considered here. Indeed, we believe that our results extend to all gauge theories in their Coulomb phase at strong coupling, thereby opening a window of understanding to a variety of physical problems in different settings.

ACKNOWLEDGMENTS

We thank S.J. Rey for a stimulating discussion at the beginning of this work, explaining to us the details of his published results. This work was supported in parts by the US-DOE grant DE-FG-88ER40388.

[1] E.V. Shuryak and I. Zahed, hep-ph/0307267.
[2] J. Maldacena, Adv. Theor. Math. Phys. **2**, 231 (1998); Phys. Rev. Lett. **80**, 4859 (1998) and references therein.
[3] S.-J. Rey and J.-T. Yee, Eur. Phys. J. C **C22**, 379 (2001).
[4] S.-J. Rey, S. Theisen, and J.-T. Yee, Nucl. Phys. **B527**, 171 (1998); A. Brandhuber, N. Itzhaki, J. Sonnenschein, and S. Yankielowicz, Phys. Lett. B **B434**, 36 (1998).
[5] M. Rho, S.J. Sin, and I. Zahed, Phys. Lett. B **466**, 199 (1999).
[6] R.A. Janik and R. Peschanski, Nucl. Phys. **B565**, 193 (2000).
[7] J. Polchinski and M.J. Strassler, Phys. Rev. Lett. **88**, 031601 (2002).
[8] G.T. Horowitz and A. Strominger, Nucl. Phys. **B360**, 197 (1991); S.S. Gubser, I.R. Klebanov, and A.A. Tseytlin, *ibid.* **B534**, 202 (1998); C.P. Burgess, N. R. Constable, and R.C. Myers, J. High Energy Phys. **99**, 9908 (1999); C. Kim and S.J. Rey, Nucl. Phys. **B564**, 430 (2000).
[9] G. Policastro, D.T. Son, and A.O. Starinets, Phys. Rev. Lett. **87**, 081601 (2001).
[10] A.O. Starinets, Phys. Rev. D **66**, 124013 (2002).
[11] D. Teaney, ''Real-time correlator of stress tensors for $\mathcal{N}=4$ SUSY YM theory in strong coupling'' (in progress).
[12] J. Erickson, G.W. Semenoff, and K. Zarembo, Phys. Lett. B **466**, 239 (1999); J.K. Erickson, G.W. Semenoff, R.J. Szabo, and K. Zarembo, Phys. Rev. D **61**, 105006 (2000); G.W. Semenoff and K. Zarembo, Nucl. Phys. B (Proc. Suppl.) **108**, 106 (2002).
[13] E.V. Shuryak, Zh. Eksp. Teor. Fiz. **74**, 408 (1978); Sov. Phys. JETP **47**, 212 (1978); Phys. Rep. **61**, 71 (1980).
[14] A.M. Polyakov, Phys. Lett. **82B**, 2410 (1979).
[15] H.A. Weldon, Phys. Rev. D **61**, 036003 (2000).
[16] P. Petreczky, F. Karsch, E. Laermann, S. Stickan, and I. Wetzorke, Nucl. Phys. B (Proc. Suppl.) **106**, 513 (2002).
[17] T.H. Hansson and I. Zahed, Phys. Lett. B **309**, 385 (1993).
[18] E.V. Shuryak, Phys. Lett. **78B**, 150 (1978); Yad. Fiz. **28**, 796 (1978).
[19] T. Matsui and H. Satz, Phys. Lett. B **178**, 416 (1986).
[20] F. Karsch, M.T. Mehr, and H. Satz, Z. Phys. C **37**, 617 (1988).
[21] S. Datta, F. Karsch, P. Petreczky, and I. Wetzorke, Nucl. Phys. B (Proc. Suppl.) **119**, 487 (2003).
[22] F. Karsch, S. Datta, E. Laermann, P. Petreczky, S. Stickan, and I. Wetzorke, Nucl. Phys. **B715**, 701 (2003).
[23] E.V. Shuryak, Nucl. Phys. **B198**, 83 (1982).